Insect Biochemistry and Molecular Biology 105 (2019) 1–9

Contents lists available at ScienceDirect

Insect Biochemistry and Molecular Biology

journal homepage: www.elsevier.com/locate/ibmb

GC/MS-based metabolomics analysis reveals active fatty acids biosynthesis in the Filippi's gland of the silkworm, *Bombyx mori*, during silk spinning

Xin Wang[a,b], Yi Li[a], Qingsong Liu[a], Xiaoyin Tan[a], Xiaoqian Xie[a], Qingyou Xia[a,b], Ping Zhao[a,b,*]

[a] State Key Laboratory of Silkworm Genome Biology, Southwest University, Chongqing, 400715, PR China
[b] Key Laboratory of Sericultural Science of Chongqing, Chongqing Engineering and Technology Research Center for Novel Silk Materials, Southwest University, Chongqing, 400715, PR China

ARTICLE INFO

Keywords:
GC-MS
Metabolomics
Filippi's gland
Silk spinning
Fatty acids biosynthesis

ABSTRACT

The Filippi's gland, also called the Lyonet's gland, is in truth a pair of tiny glands that are unique to lepidopteran insects. Although the ultrastructure of the Filippi's gland has been well-understood, the specific biological function of this gland in silk spinning is still unclear. Previous studies proposed a hypothesis that this gland might synthesize and secrete some substances into the anterior silk gland (ASG) to help silk spinning. In order to identify these metabolites, a GC/MS-based metabolomics technique was introduced. A total of 59 metabolites, including fatty acids, amino acids, and sugars, were identified in glands from silkworm larvae in the feeding and silk spinning stages. Abundance and pathway analyses revealed that these metabolites had different abundances during gland development and silk spinning, which may facilitate the transport of small molecules and ions. The most interesting result is that the Filippi's gland has a very active fatty acid biosynthesis process during spinning, suggesting that it may synthesize lipids or waxes and secrete them into the ASG to promote silk spinning. This data provides instructive insight into the biological functions of Filippi's gland from both silkworms and other lepidoptera.

1. Introduction

The silkworm, *Bombyx mori*, is a lepidopteran insect with important economic value. The silk fiber produced by silkworm larvae has attracted great attention because of its good mechanical properties and biocompatibility (Huang et al., 2018; Omenetto and Kaplan, 2010; Vepari and Kaplan, 2007). Silk fiber is synthesized and secreted by a pair of specialized organs in the silkworm body known as the silk gland (Xia et al., 2014). The silk gland can be divided into posterior silk gland, middle silk gland, anterior silk gland, and spinneret based on both morphological and functional differences (Wu, 1980). Silk fibroin, the most important component of silk fiber, is synthesized in the posterior silk gland. Sericin, produced in the middle silk gland, seals the silk filaments into the fiber and provides the sticky fiber coating. The anterior silk gland forms a duct through which silk flows to form a solid silk fiber in the spinneret. At present, the anterior silk gland and spinneret are considered as the loci for silk fibrillogenesis (Chang et al., 2015; Wang et al., 2017b; Yi et al., 2013).

In addition to these four main sections, there are also small accessory glands present in the silk gland, the most representative of which is known as Filippi's (or Lyonet's) gland. This gland, which is unique to lepidoptera (Machida, 1965), was discovered as early as the 1760s, but to date, research has focused solely on morphological and ultrastructural descriptions (Waku and Sumimoto, 1974).

The Filippi's gland is grape-like in shape and is connected by a small duct to the common duct of the spinneret. Through transmission electron microscopy, researchers observed the ultrastructure of the Filippi's gland. The gland cells were characterized by the presence of complicated canaliculi bearing microvilli on their inner surface, large numbers of mitochondria and free ribosomes, and a remarkably convoluted basal plasma membrane (Victoriano and Gregorio, 2004; Waku and Sumimoto, 1974). However, the gland cells lack the well-developed cytoplasmic membrane system such as rough- and smooth-surfaced endoplasmic reticula and Golgi bodies (Victoriano and Gregorio, 2004; Waku and Sumimoto, 1974) which are required for gland function.

Although the ultrastructure of the Filippi's gland is now well-

Abbreviations: GC-MS, gas chromatography-mass spectrometry; ASG, anterior silk gland; QC, quality control; EI, electron impact; m/z, mass-to-charge; RT, retention time; NIST, National Institute of Standards and Technology; OPLS-DA, orthogonal partial least squares discriminant analysis; KEGG, Kyoto Encyclopedia of Genes and Genomes; qRT-PCR, quantitative real-time polymerase chain reaction; TIC, total ion chromatograms

* Corresponding author. State Key Laboratory of Silkworm Genome Biology, Southwest University, Chongqing, 400715, PR China.
E-mail address: zhaop@swu.edu.cn (P. Zhao).

https://doi.org/10.1016/j.ibmb.2018.12.009
Received 19 July 2018; Received in revised form 14 December 2018; Accepted 16 December 2018
Available online 18 December 2018
0965-1748/

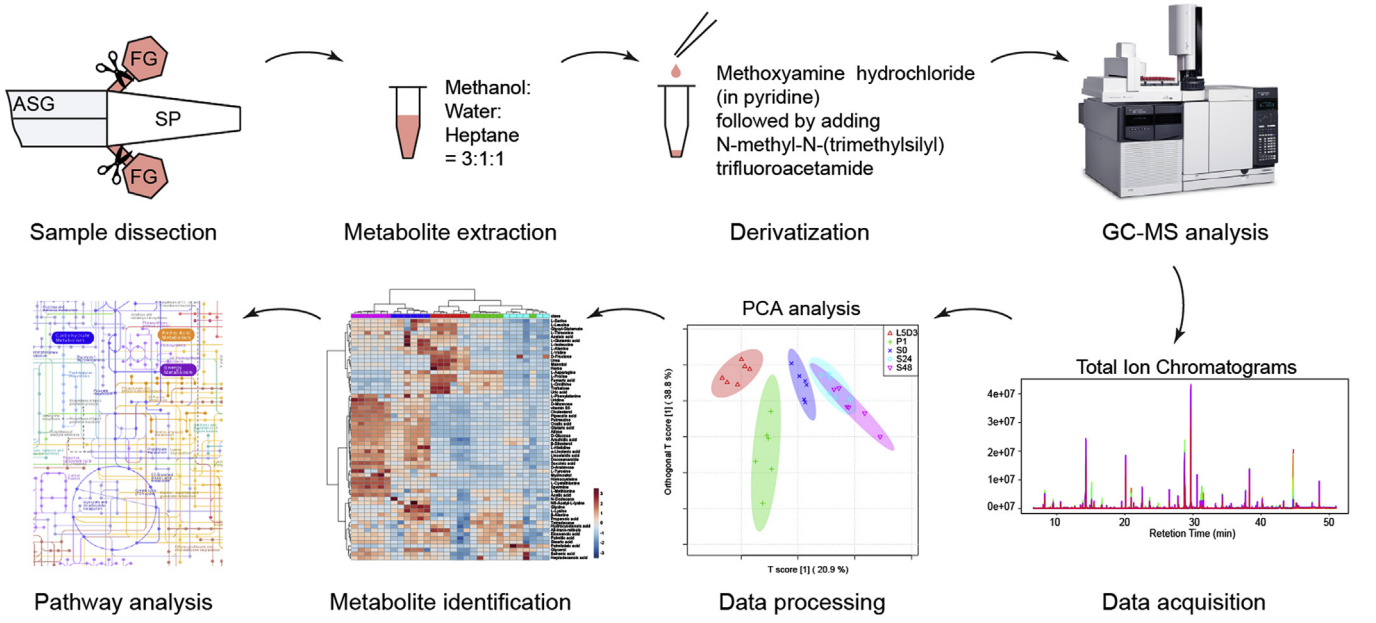

Fig. 1. Work-flow of this study. The Filippi's glands were dissected and their metabolites extracted in a mixture of methanol, heptane and water. After incubation with methoxyamine hydrochloride and N-methyl-N-(trimethylsilyl) trifluoroacetamide, derivatized metabolites were analyzed via GC-MS. The metabolomics data were obtained and processed by the local and online software. We then compared the abundances to find the differential metabolites. Finally, the pathways in which the identified metabolites and differential metabolites involved were also studied, assisted by KEGG online tools. ASG, anterior silk gland; SP, spinneret; FG, Fillip's gland.

understood, the specific biological function of the gland during silk spinning remains unknown. At present, there are many hypotheses concerning the function of the Filippi's gland, with some suggesting that it may secrete a lubricant into the anterior silk gland to help with spinning (Glasgow, 1936). This study used a GC/MS-based metabolomics technique—widely used in recent contemporary silkworm research (Chen et al., 2015; Dong et al., 2017; Li et al., 2016a, 2016b; Zhou et al., 2015)—to identify the metabolites present in the Filippi's gland of silkworms at different developmental stages. These results fully demonstrate that metabolomics is a powerful technique for studying the function of the specific tissues. Fig. 1 provides an overview of the general methods employed in metabolomics research, along with the modifications made to it in our study. Experimental procedures include tissue dissection, extraction and derivatization of metabolites, GC-MS analysis, data acquisition and pretreatment, metabolite identification, differential analysis, and metabolic pathway analysis.

2. Materials and methods

2.1. Insects

Silkworm (Strain: p50) larvae were provided by the State Key Laboratory of Silkworm Genome Biology (Southwest University, China), and were raised on mulberry leaves in standard conditions (26 °C, 75% RH). The Filippi's glands used in this study were collected from silkworms on the third day of the fifth instar (L5D3), and from those in the wandering stage at 12 h intervals—ws0h (silkworm is about to spin silk), 12 h (ws12h), 24 h (ws24h), 36 h (ws36h), and 48 h (ws48h).

2.2. Sample collection

Larval silkworm spinnerets were carefully dissected under a microscope at the aforementioned time points. In the spinneret, the Filippi's gland is located in the common duct where the two anterior silk gland ducts join. The clean Filippi's gland was obtained by cutting at a point slightly distal to the connection of the common and Filippi's gland ducts (Wang et al., 2016). Each sample contains 50 Filippi's glands with 6 biological replicates.

2.3. Metabolite extraction and derivatization

Each sample was homogenized in 500 μL of a methanol-hexane-water (3:1:1) mixture and sonicated for 15 min, followed by incubation on ice for 30 min. After this, the sample was centrifuged at 18000 rpm for 30 min at 4 °C, and the supernatant collected and dried in a vacuum concentrator. The dry metabolites were dissolved in 50 μL of pyridine containing 20 mg/mL methoxylamine hydrochloride. After sonication for 15 min, the sample was incubated at 70 °C for 30 min. Then, 50 μL of N-methyl-N-(trimethylsilyl) trifluoroacetamide was added and the sample incubated at 70 °C for 30 min. During this process, the metabolites are trimethylsilylated, thus we added 10 μL of hexane to stop the reaction. The sample was then centrifuged at 18000 rpm for 30 min and the supernatant used for GC-MS analysis. We also prepared the quality control (QC) samples by pooling 10 Filippi's glands from each time point with the same processing method.

2.4. GC-MS analysis

The sample (1 μL) was auto-injected at a 1:10 split ratio into a 7890B/5977A GC-MS (Agilent) equipped with a HP-5MS column (length 30 m, i.d. 0.25 mm; Agilent). The temperatures of inlet, transfer interface and ion source were set at 300, 280, and 230 °C respectively. The oven temperature was set as follows: initiate at 70 °C and hold for 3 min, elevate to 140 °C at a rate of 5 °C/min, to 200 °C at 4 °C/min, to 240 °C at 5 °C/min, ramp to 300 °C at a rate of 10 °C and hold for 3 min. Detector voltage was set to 0.93 kV, and the EI ionization voltage of the metabolites was 70 eV. Mass spectra were recorded from 50 to 550 *m/z*.

2.5. Data preprocessing and analysis

Raw data files were converted into AIA data format and sent to XCMS online (https://xcmsonline.scripps.edu/index.php). The metabolic peaks were identified by comparing their mass spectra with both

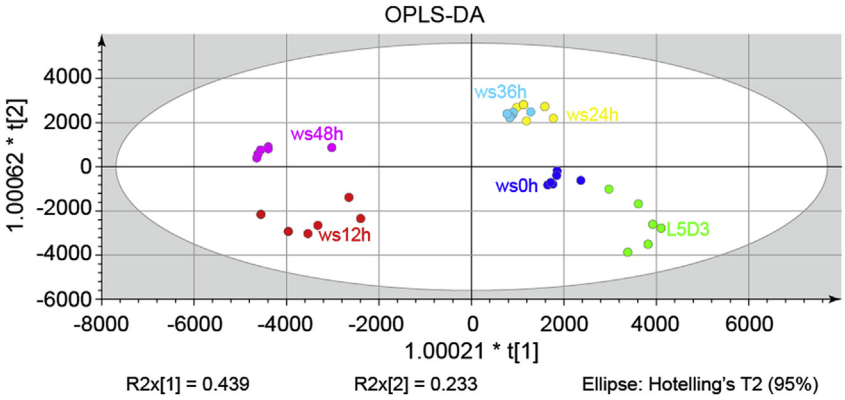

Fig. 2. OPLS-DA of identified metabolites between samples (with six biological replicates).

the NIST 2011 (version 2.0, National Institute of Standards and Technology, USA) library and standard compounds. Only a relative score over 700 was considered to be a good match. Orthogonal partial least squares discriminant analysis (OPLS-DA) (Boccard and Rutledge, 2013) was performed using SIMCA-P software (version 14.0) to obtain the separated trend of sample sets. In order to show patterns of metabolite abundance in different samples, a heat map was created by using MetaboAnalyst online software (http://www.metaboanalyst.ca/faces/home.xhtml) (Xia et al., 2015). To reveal the metabolic differences of Filippi's gland between feeding and spinning stages, the metabolites identified in L5D3 and ws12h were subjected to differential analysis. Differential metabolites were identified following the method described previously (Li et al., 2016b), with only metabolites that changed ≥ 1.5-fold (enriched metabolites) or ≤ 0.65 (decreased metabolites) in relative ratios (p-value < 0.05) considered to be significantly altered.

2.6. Pathway analysis

All the identified metabolites were submitted to the Kyoto Encyclopedia of Genes and Genomes (KEGG) pathway database (http://www.kegg.jp/kegg/pathway.html). The KEGG ID and the pathways in which the metabolites are involved were obtained. Metabolites that were not identified in the database were not used for further analysis. Pathway enrichment was performed using the Metabolomics Pathway Analysis (MetPA) program, integrated into MetaboAnalyst online software (Xia and Wishart, 2010). The differential metabolites were uploaded, with the *Drosophila melanogaster* pathway library used as the reference library. The algorithms used applied hypergeometric tests for over representation analysis and out-degree centrality for pathway topology analysis.

2.7. RNA isolation, cDNA synthesis and qRT-PCR analysis

Total RNAs from the Filippi's gland on 3rd day of fifth instar (L5D3) and 12 h into wandering (ws12h) were extracted using TRIzol Reagent (ThermoScientific, USA) and reverse transcribed using GoScript Reverse Transcription System (Promega, USA) according to the manufacturer's protocol. Genes related to the fatty acids pathway were selected via the KEGG pathway database (pathway No. map01040, map00561) and our previous transcriptome data (Wang et al., 2016). The details of these genes are listed in Table S1. Sequences of the primers corresponding to the selected genes were identified from the qPrimerDB database (Lu et al., 2018). Primer pairs were synthesized by Sangon Biotech (China) and used for qRT-PCR amplification as previously described (Wang et al., 2017a), with amplified products detected using SYBR-Green Supermix (TaKaRa, Japan) with a 7500Fast Thermal Cycler (ThermoScientific, USA). The expression level of the silkworm transcription initiation factor 4a (*Tif4a*) gene was used as an internal control (Wang et al., 2008), with gene expression levels normalized to the *Tif4a* controls from three independent experiments.

As our previous study had found that the genes encoding transporters are enriched in the Filippi's gland and responsible for small solute transportation (Wang et al., 2016), we also determined their expression in the Filippi's gland. Details of these genes are listed in Table S2.

3. Results

3.1. Metabolites in the silkworm's Filippi's gland

In this work, the metabolomics of silkworm Filippi's gland from feeding (L5D3) and spinning silkworms (ws0h, ws12h, ws24h, ws36h, ws48h) were analyzed. Using GC-MS, a total of 59 metabolites were identified (Table S3). Total ion chromatograms (TICs) of different samples are shown in Fig. S1. Among the 59 metabolites were 21 amino acids, 10 fatty acids, 9 organic acids, 6 sugars, 5 sterols and lipids, 2 alkanes, with the remainder categorized as unclassified metabolites. OPLS-DA analysis showed a clear separation between samples except for ws24h and ws36h (Fig. 2). This result implies that the metabolic characters between these time points are different. However, the ws24h and ws36h Filippi's gland samples share similar metabolic characters. Due to the similar metabolic character of the ws24h and ws36h Filippi's gland samples, ws36h sample was not used in further analysis.

In order to observe patterns of metabolite abundance overall, we performed a hierarchical clustering analysis. A heat-map based on the abundance of the identified metabolites is shown in Fig. S2. As can be seen in Fig. S2, amino acids, such as serine, alanine, leucine, iosleucine, valine, threonine, and glutamic acid, are abundant in L5D3 and ws12h samples. However, fatty acids, such as arachidic acid, α-linolenic acid, linoelaidic acid, heptadecanoic acid, palmitic acid, stearic acid, and docosanoic acid are more common in the ws48h sample.

3.2. Pathways in which the identified metabolites are involved

The metabolites were located in the KEGG database and thus determined the pathways in which Filippi's gland metabolites are involved. In total, there are 59 metabolites which participate in 166 pathways (Table S4), of which, 40 are involved in metabolic pathways, suggesting a very high metabolic rate in the gland (Fig. 3). When we observed the metabolic pathways carefully, we found that the biosynthesis and metabolism of amino acids, fatty acids, and other secondary metabolites are prominent. There are 23 metabolites involved in the ABC transporter pathway (ko02010), which suggests that transportation processes are also active in Filippi's gland.

In Fig. 3, we also found some interesting clues that 13 metabolites are involved in mineral absorption (ko04978). This evidence suggests metal ions might be present in Filippi's gland. It should be noted that there are 6 metabolites which participate in the biosynthesis of

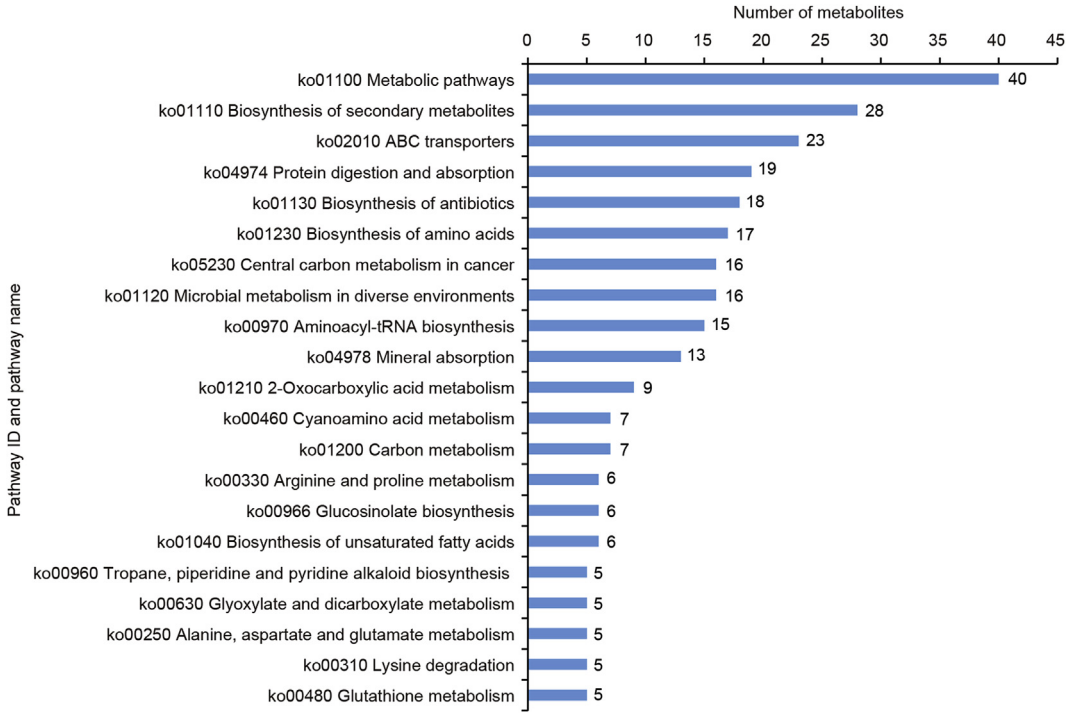

Fig. 3. Pathway analysis of the identified metabolites (metabolites number ≥ 5).

unsaturated fatty acids (ko01040). This pathway is of particular note, and we will discuss it in detail later in this article.

3.3. Differential analysis of the identified metabolites

In order to highlight the metabolic differences in the glands between the spinning and feeding stages, differential analysis was performed using data from ws12h and L5D3. There were 34 differential metabolites identified, of which 28 were enriched and 6 were decreased in the spinning stage (Table 1). The metabolites enriched during spinning are amino, fatty, and organic acids, while the decreased metabolites are urea, uric acid, and sugars.

Furthermore, pathway enrichmental analysis of differential metabolites were studied using the MetPA program, with the results showing that differential metabolites are enriched in 44 pathways. Among them, 12 pathways are significantly enriched ($p < 0.005$ and FDR < 0.003), including sugar metabolism (amino sugar, fructose, mannose and galactose), pentose phospate pathway, amino acid metabolism (lysine, β-alanine, arginine and proline), steroid biosynthesis, pyrimidine metabolism, α-linolenic acid metabolism, and aminoacyl-tRNA biosynthesis (Fig. 4).

3.4. Abundance analysis of sugars and amino acids

In Fig. 4, we can easily find that the levels of sugars and amino acids changed between spinning and feeding. To further evaluate these differences, an abundance analysis of these two kinds of metabolites was performed.

Abundance analysis of sugars in Filippi's gland is shown in Fig. 5. Whilst, trehalose and fructose are abundant during feeding, both decrease during spinning. This contrasts with glucose, arabinose and mannose levels which remain low during the feeding stage, but are enriched during spinning process. Trehalose is the blood sugar of silkworm (Wu, 1980), and since its level decreases while that of glucose increases during spinning, we suggest trehalose has been hydrolyzed to form glucose, which can then be used to provide sufficient energy for the transportation of small solutes during spinning.

Table 1
Metabolite differentials between spinning and feeding stages.

Metabolites	Catergory	*p*-value	Fold Change
Up-regulated (ws12h verses L5D3)			
Homocysteine	Amino acid	0.007	62.38
D-Glucose	Sugar	< 0.001	34.34
Allose	Sugar	< 0.001	34.05
Putrescine	Polyamine	0.003	17.86
D-Mannose	Sugar	< 0.001	9.87
N6-Acetyl-L-lysine	Amino acid	0.003	7.03
Glutaric acid	Organic acid	< 0.001	6.85
L-Lysine	Amino acid	0.001	6.57
β-Alanine	Amino acid	< 0.001	4.77
Pipecolic acid	Organic acid	0.009	4.42
L-Phenylalanine	Amino acid	0.012	4.02
Uridine	Nucleoside	0.002	3.72
L-Histidine	Amino acid	0.004	3.65
L-Glycine	Amino acid	0.006	3.51
vitamin B5	Organic acid	< 0.001	3.44
Oxalic acid	Organic acid	< 0.001	3.31
Cholesterol	Sterol and lipid	< 0.001	2.80
Linoelaidic acid	Fatty acid	0.002	2.31
Docosanamide	Fatty acid amide	0.002	2.30
Spermine	Amide	0.027	2.26
β-Sitosterol	Sterol and lipid	0.001	2.11
L-Cystathionine	Amino acid	< 0.001	1.97
α-Linolenic acid	Fatty acid	0.001	1.85
Arachidic acid	Fatty acid	0.005	1.77
Behenic acid	Fatty acid	0.039	1.77
L-Asparagine	Amino acid	0.048	1.62
N-Dodecane	Alkane	0.045	1.61
D-Arabinose	Sugar	0.005	1.60
Down-regulated (ws12h verses L5D3)			
Uric acid		0.042	0.47
Urea		< 0.001	0.44
Trehalose	Sugar	0.032	0.42
D-Fructose	Sugar	< 0.001	0.19
Mannitol	Sterol and lipid	0.001	0.19
Heme	Ion binding	0.001	0.13

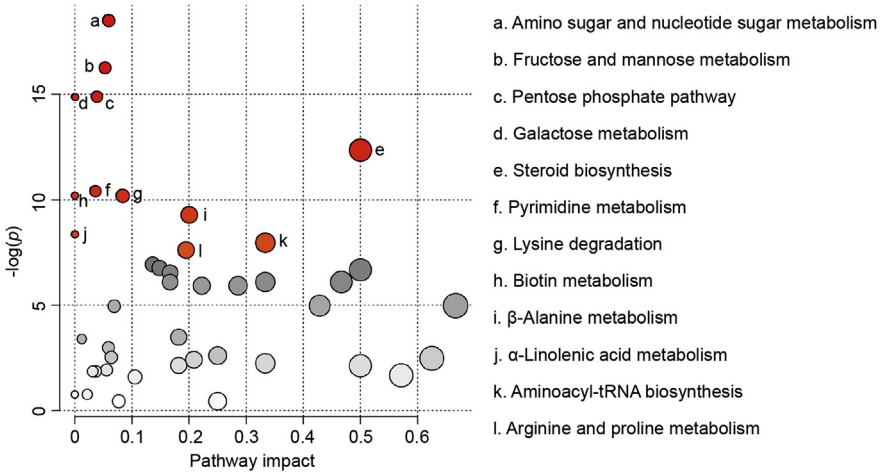

Fig. 4. Pathway enrichmental analysis of differential metabolites using MetPA program (http://www.metaboanalyst.ca/faces/home.xhtml). The colored plots represent the most significant enriched pathways (p-value < 0.005, FDR < 0.003). The deeper the red color of the pathway, the bigger the significant difference of the metabolic pathway. (For interpretation of the references to color in this figure legend, the reader is referred to the Web version of this article.)

Further, we analyzed the abundance of 15 identified amino acids and found that their abundance can be classified into four categories (Fig. 6). The first category contains aspartic acid, glycine, lysine, histidine, methionine, and phenylalanine. Such amino acids accumulate gradually from L5D3 to ws12h and decrease during the later stage of spinning. The second category includes alanine, leucine, isoleucine, valine, serine, and glutamate, which have higher levels in L5D3 and ws12h. The third category contains proline and threonine, and their abundances diminish gradually. Tyrosine is to be classified in a fourth category, whose abundance is inversely proportional to that of the third. With the growth and development of the Filippi's glands, tyrosine gradually accumulates in the silk spinning process and reaches its maximum content at the end of spinning. Like the silk glands, the Filippi's gland begins to develop during the fifth instar, reaching maturity in the early stages of spinning, and undergoes tissue degradation at the end of spinning (Patra et al., 2012). Changes in the amino acids shown in Fig. 6 indicate possible protein synthesis in the fifth instar and proteolysis at the end of spinning in Filippi's gland.

In our previous paper, we found that many transporting protein genes were enriched in the Filippi's gland (Wang et al., 2016). Most of these genes are related to the transport of small solutes such as sugar, amino acids, and ions (Table S2). To make clear whether these genes were expressed in the Filippi's gland, we performed qRT-PCR analysis. Fig. 7 shows the expression levels of these genes. As these genes are indeed expressed in the Filippi's gland, and because most of them are up-regulated during silk spinning, it is likely that they play roles in small solute transport. This conclusion is supported by evidence from both the transcriptome and metabolome analyses.

3.5. Abundance and pathway analysis of fatty acids

Previous research had suggested that the Filippi's gland may secrete some kind of lubricant into the anterior silk gland to help silk spinning. Lubricants are typically esters such as greases, lipids, and waxes, but since GC-MS vaporizes metabolites at high temperatures for metabolite separation and detection, and esters are hard to volatilize at high temperature, we failed to detect any esters in this study.

Fatty acids are the precursors of esters, and we detected large numbers of them in the Filippi's gland. The abundance analysis of fatty acids is shown in Fig. 8A. According to the abundance pattern, these metabolites can be classified into 2 categories. The first category contains arachidic acid, α-linolenic acid, linoelaidic acid, heptadecanoic acid, and docosanoic acid. These fatty acids accumulate gradually during spinning. The second category is those where the abundance during spinning is essentially constant. This category includes palmitoleic acid, palmitic acid, and stearic acid. In addition, we also found that the abundance of fatty acids from either the first or the second category at each time point during spinning was higher than the abundance in the feeding stage (Fig. 8A), implying that fatty acid metabolisms are active in spinning stage.

Esters are formed by the dehydration condensation of glycerol and fatty acids, so we also investigated the abundance of glycerol in the Filippi's gland. During spinning, the glycerol content in the Filippi's gland gradually increases, yet its abundance at each time point during spinning remains higher than that in the feeding stage (Fig. 8A).

We analyzed the biological pathways in which fatty acids and glycerol are involved, finding that these metabolites are enriched in the biosynthesis of unsaturated fatty acids (n-3 family), lipid metabolism,

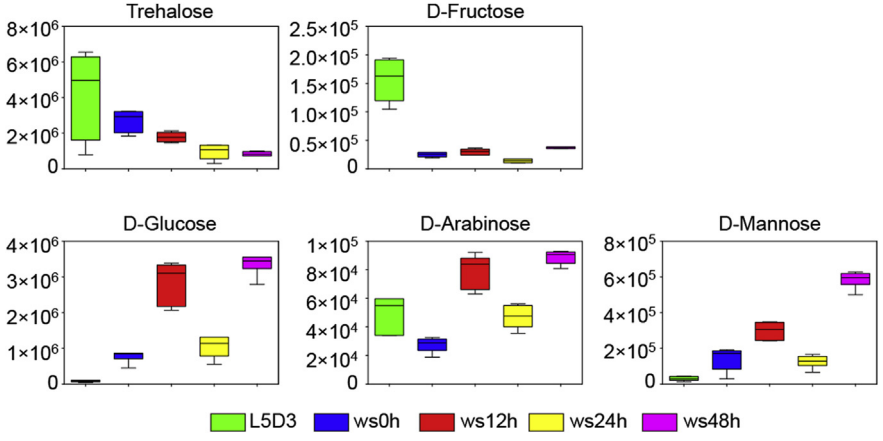

Fig. 5. Abundance analysis of the sugars identified in Filippi's glands from different developmental stages.

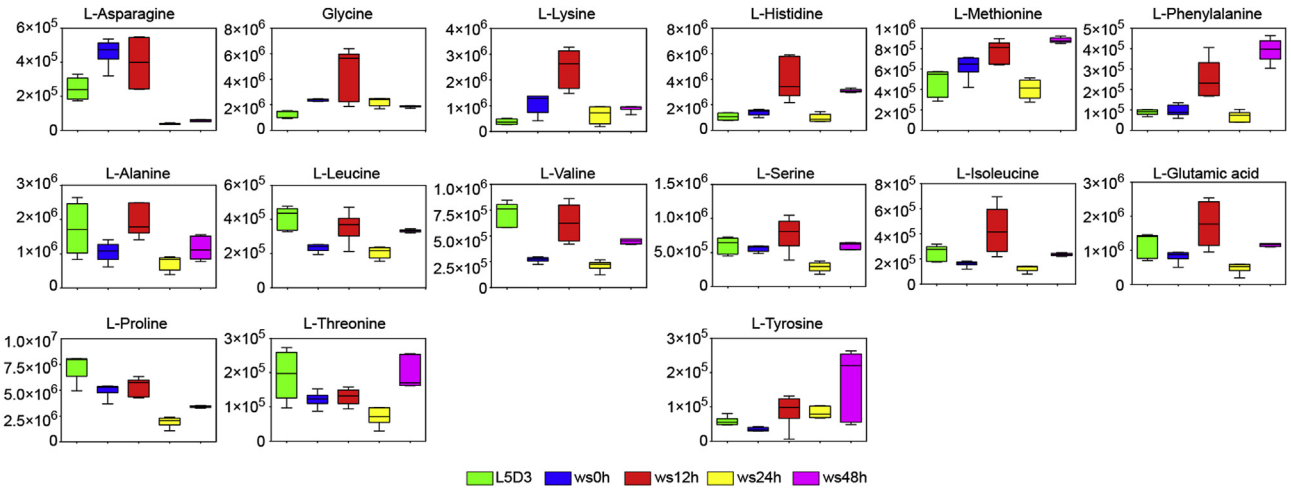

Fig. 6. Abundance analysis of the 15 amino acids identified in Filippi's glands from different developmental stages.

and cutin, suberine and wax biosynthesis pathways. To further confirm whether these pathways are actually present in the Filippi's gland, we first selected the genes involved in these pathways using KEGG online tools and our previous transcriptomic data before using qRT-PCR to determine their expression in the gland. Detailed information of the relative expression levels of these genes are shown in Table S1 and Fig. 8B. The genes encoding enzymes and transporters within these pathways, such as fatty acid synthase (EC: 2.3.1.85), glycerol kinase (EC: 2.7.1.30), palmitoyl-CoA hydrolase (EC: 3.1.2.2), fatty acid transport protein, and fatty acid binding protein, were expressed in the Filippi's gland. Furthermore, some of the genes encoding key regulatory enzymes (EC: 2.3.1.85, EC: 2.7.1.30, EC: 3.1.2.2) were up-regulated during silk spinning. All of which confirms that the pathways for fatty acid biosynthesis are present and active in the Filippi's gland during silk spinning.

To identify the metabolites and genes in their metabolic pathways, a schematic diagram was drawn (Fig. 9). The identified fatty acids all participate in the biosynthetic pathway of unsaturated fatty acids as substrates or products. Among them, palmitic acid, docosanoic acid, arachidic acid, α-linolenic acid, eicosenoic acid, and stearic acid are able to react with glycerol and enter the lipid metabolism pathway to synthesize triacylglycerol. In addition, palmitic acid and docosanoic acid can also be used as substrates to participate in the cutin, suberine and wax biosynthesis pathway. Since docosanoic acid, arachidic acid, α-linolenic acid and glycerol all accumulate in the spinning process, it is reasonable to speculate that a large number of lipid or wax metabolites may be synthesized during spinning. This suggests that there is an active ester synthesis process in the Filippi's gland, and that synthesized ester metabolites very likely participate in the spinning process as a lubricant.

4. Discussion

In this study, we reported the GC/MS-based metabolomics profiles of the Filippi's gland of silkworm larvae at different developmental stages. Then, we systematically analyzed the abundance changes of these metabolites and the biological pathways these metabolites involved in. A total of 59 metabolites were identified in this study (Table S3), including amino acids, fatty acids, and sugars. The identified metabolites have different abundance changes, which may be related to

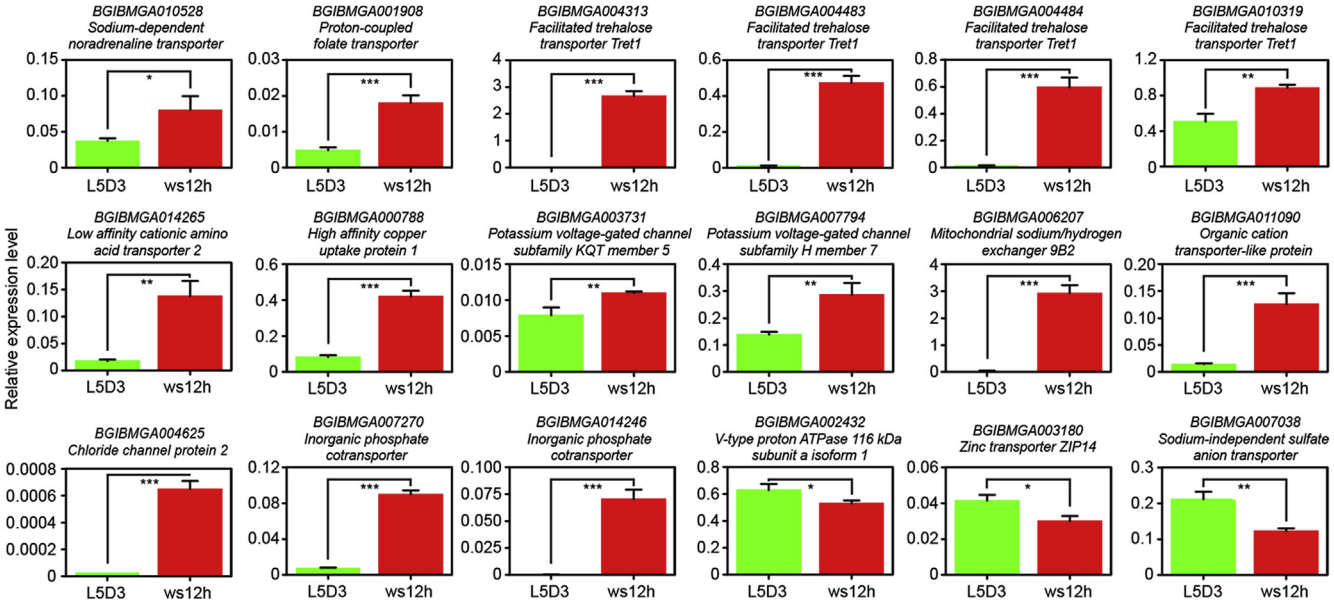

Fig. 7. The relative expression levels of the genes encoding transporters in the Filippi's gland. These genes were identified from previous transcriptomics data (Wang et al., 2016) and their details are listed in Table S2.

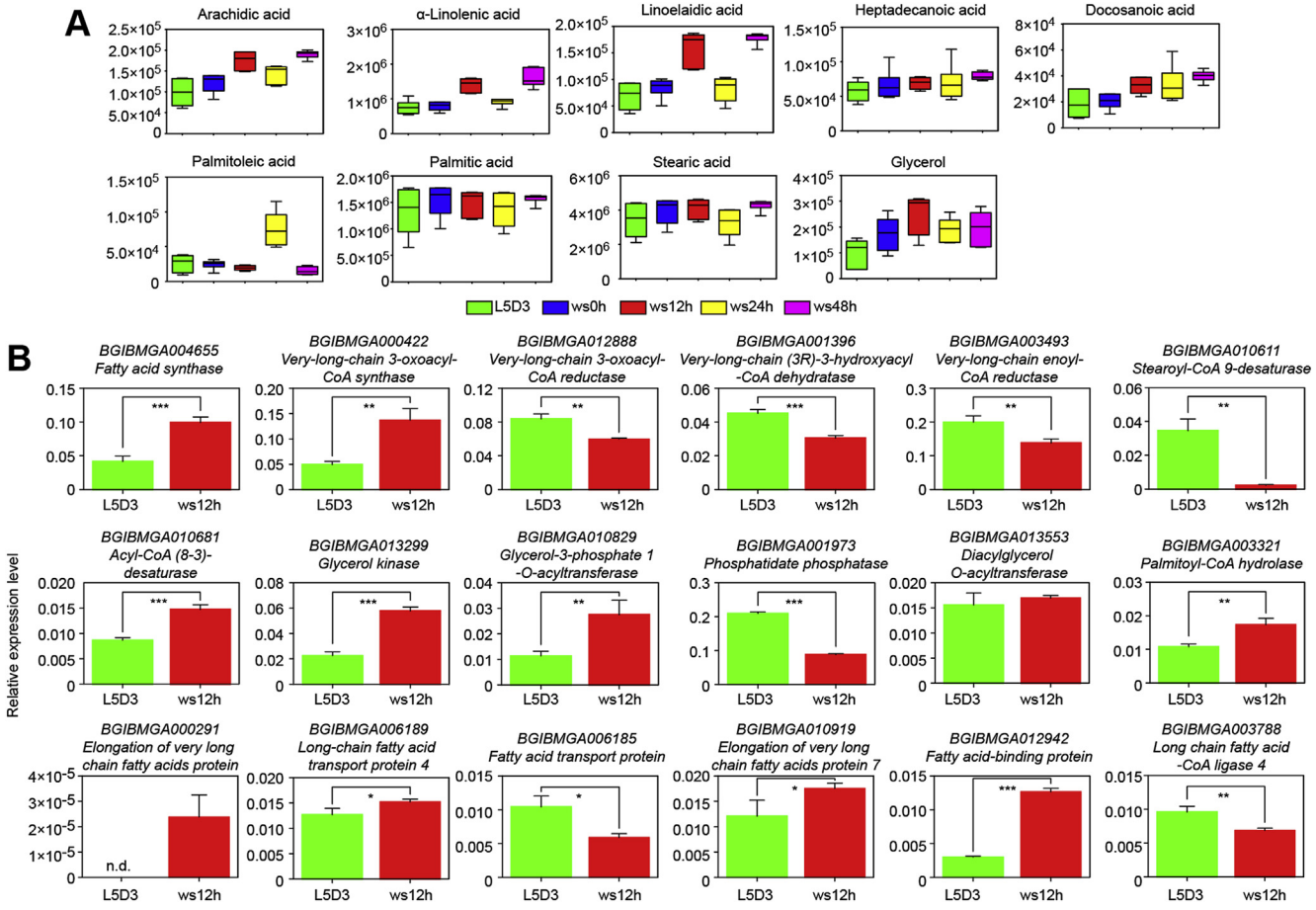

Fig. 8. Abundance analysis of the fatty acids identified from different developmental stages (A) and the relative expression levels of the genes related to fatty acids biosynthesis (B). These genes were identified from the KEGG database and our previous transcriptomics data (Wang et al., 2016). The details of these genes are listed in Table S1.

the differences in the specific biological pathways in which they participate. The most interesting result is that the Filippi's gland has a very active fatty acid biosynthesis process during spinning (Fig. 9), suggesting that the Filippi's gland may produce lipids or waxes through ester synthesis pathways and secrete them into the anterior silk gland to facilitate silk spinning.

The Filippi's gland is an organ whose presence has been known for more than 3 centuries, but the depth of study into its physiological functions is limited compared to this. Until today, researchers have maintained various hypotheses as to its function. As early as 1876,

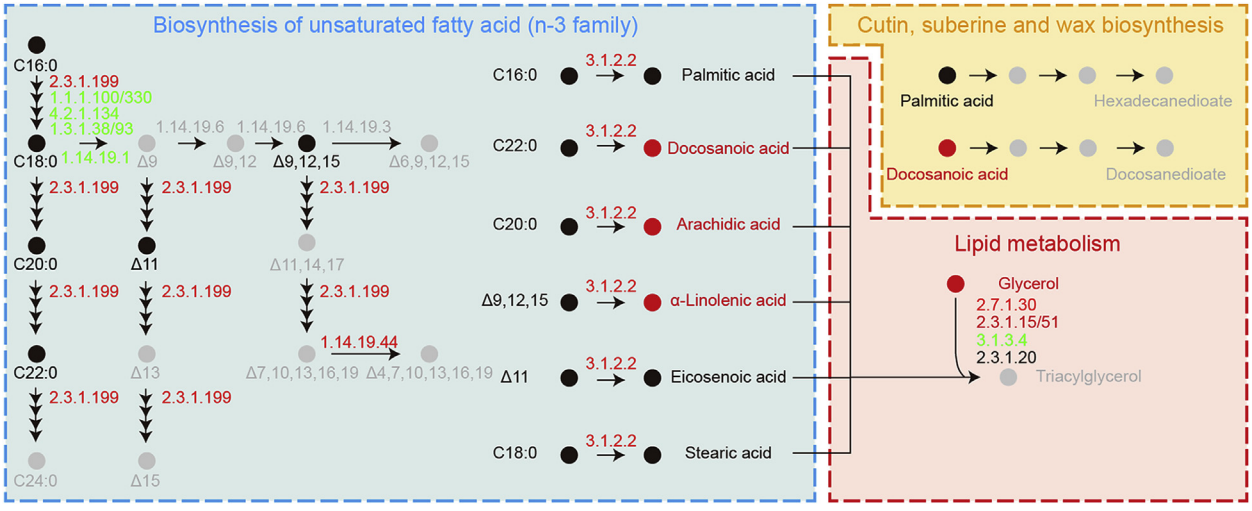

Fig. 9. Pathways in which the identified metabolites are involved. Black and red points represent identified metabolites, red points are significant enriched metabolites, and grey points represent unidentified metabolites. The EC (Enzyme Commission) numbers of the enzymes participating in these pathways are also shown in colored letters (the red represents up-regulated genes, the green represents down-regulated genes, and the black represents un-regulated genes). (For interpretation of the references to color in this figure legend, the reader is referred to the Web version of this article.)

Helm (1876) proposed that the Filippi's gland may secrete some kind of "adhesive" onto silk proteins, thereby fusing the two filaments together. Later, it was proposed that the Filippi's gland secretes a "lubricant" to promote silk spinning (Glasgow, 1936). After careful examination of the ultrastructures of this gland, others proposed that the Filippi's gland has no function because its gland cells lack a well-developed cytoplasmic membrane system (Drecktrah et al., 1966; Sorour et al., 1990). In 1997, Zhang et al. compared the morphology of Filippi's glands from 18 lepidopteran species and surmised that the Filippi's gland is vestigial and does not affect silk spinning (Zhang et al., 1997). On the other hand, our group reported the transcriptomic data of silkworm spinneret and Filippi's gland in 2016 (Wang et al., 2016), wherein many genes associated with small solute transport were identified. In this work, we further proved that these genes were indeed expressed in the Filippi's gland and up-regulated during silk spinning (Fig. 7). Thus, we suggest that the Filippi's gland is active in transporting small solutes such as ions, sugars and amino acids to the silk gland (Wang et al., 2016), and that these ions, sugars and amino acids are vital for silk fiber formation (Wang et al., 2017a). This is the first time that molecular biologial methods have been used to study the Filippi's gland, but our data supports the hypothesis which Waku and Sumimoto (1974) proposed—that the Filippi's gland is responsible for the transport of small molecules into the silk gland lumen. In this study, we found that 23 metabolites are involved in the ABC transporter pathway and 13 are involved in the mineral uptake pathway, which provides further support for their hypothesis.

There is still no clear evidence as to whether the Filippi's gland synthesizes lubricating substances for use in the silk gland. Ultrastructural analysis revealed that the inner surface of gland cells contains complex microvilli composed of microtubules. The gland cells also have large numbers of mitochondria and free ribosomes, and a remarkably convoluted basal plasma membrane (Victoriano and Gregorio, 2004; Waku and Sumimoto, 1974), suggesting that they have the structural and energetic basis for lubricant synthesis. It has been reported previously that a large number of secretory granules containing proteins, glycogen and lipids have been detected in the Filippi's gland cells from the tropical tasar silkworm, *Antheraea mylitta* (Patra et al., 2012). In our current study, we also found that a large number of amino acids, sugars and fatty acids are present in the Filippi's gland from the domesticated silkworm, *Bombyx mori* (Table S3 and Figs. 5, 6 and 8). The genes involved in fatty acid biosynthesis pathways were also expressed in the gland (Fig. 8B and Table S1), indicating that the gland is indeed involved in synthesis and secretion of substances, rather than a vestigial organ without biological function. Abundance analysis of fatty acid metabolites found that a large number of related metabolites accumulate in the spinning process (Fig. 8A). Pathway analysis also revealed that these metabolites are involved in lipid metabolism, cutin, suberine and wax biosynthesis as substrates or products (Fig. 9). Furthermore, some of the genes encoding key regulatory enzymes for those pathways were up-regulated during silk spinning (Fig. 8B and Table S1). All of which suggests that the Filippi's gland may synthesize and secrete large quantities of lipids or waxy substances into the silk gland to facilitate the silk fiber spinning.

5. Conclusions

The metabolites in the Filippi's gland of silkworm larvae were systematically identified and analyzed using a GC/MS-based metabolomic technique. A total of 59 metabolites were identified in the gland. Pathway analysis showed that most of the metabolites are involved in metabolic pathways, transport processs and mineral absorption processes. Abundance analysis of fatty acid-related metabolites found that they are significantly enriched during spinning, and that these metabolites are involved in lipid metabolism and cutin, suberine and wax biosynthesis. The above results show that the Filippi's gland is metabolically active during silk spinning, and that the energy generated can facilitate the transport of small molecules and ions. Proteins, lipids or wax could also be synthesized and secreted into the silk gland to promote silk spinning. All of which provides novel insight into the biological functions of the Filippi's glands of lepidopteran insects.

Competing interests

The authors declare that they have no competing interests.

Acknowledgement

We would like to thank Mr. J. Sparkes in the University of Sheffield, UK for helping us in editing the manuscript. This work was supported by the National Natural Science Foundation [grant numbers 31472154, 31772532], the doctoral Foundation of the Southwest University [grant number SWU118052], and the special grant from post-doctoral research project in Chongqing [grant number Xm2017077].

Appendix A. Supplementary data

Supplementary data to this article can be found online at https://doi.org/10.1016/j.ibmb.2018.12.009.

References

Boccard, J., Rutledge, D.N., 2013. A consensus orthogonal partial least squares discriminant analysis (OPLS-DA) strategy for multiblock Omics data fusion. Anal. Chim. Acta 769, 30–39.
Chang, H., Cheng, T., Wu, Y., Hu, W., Long, R., Liu, C., Zhao, P., Xia, Q., 2015. Transcriptomic analysis of the anterior silk gland in the domestic silkworm (Bombyx mori) - insight into the mechanism of silk formation and spinning. PLoS One 10, e0139424.
Chen, Q., Liu, X., Zhao, P., Sun, Y., Zhao, X., Xiong, Y., Xu, G., Xia, Q., 2015. GC/MS-based metabolomic studies reveal key roles of glycine in regulating silk synthesis in silkworm, Bombyx mori. Insect Biochem. Mol. Biol. 57, 41–50.
Dong, H.L., Zhang, S.X., Tao, H., Chen, Z.H., Li, X., Qiu, J.F., Cui, W.Z., Sima, Y.H., Cui, W.Z., Xu, S.Q., 2017. Metabolomics differences between silkworms (Bombyx mori) reared on fresh mulberry (Morus) leaves or artificial diets. Sci. Rep. 7, 10972.
Drecktrah, H.K., Knight, K.L., Brindley, T.A., 1966. Morphological investigations of the european corn borer. Iowa State J. Sci. 40, 257–286.
Glasgow, J.P., 1936. Internal anatomy of a caddis (Hydropsyche colonica). Q. J. Microsc. Sci. 79, 151 151.
Helm, F.E., 1876. Ueber die Spinndrusen der Lepidopteren. Zeitsch. Wiss. Zool. 26, 434–469.
Huang, W., Ling, S., Li, C., Omenetto, F.G., Kaplan, D.L., 2018. Silkworm silk-based materials and devices generated using bio-nanotechnology. Chem. Soc. Rev. 47, 6486–6504.
Li, Y., Wang, X., Chen, Q., Hou, Y., Xia, Q., Zhao, P., 2016a. Metabolomics analysis of the larval head of the silkworm, Bombyx mori. Int. J. Mol. Sci. 17.
Li, Y., Wang, X., Hou, Y., Zhou, X., Chen, Q., Guo, C., Xia, Q., Zhang, Y., Zhao, P., 2016b. Integrative proteomics and metabolomics analysis of insect larva brain: novel insights into the molecular mechanism of insect wandering behavior. J. Proteome Res. 15, 193–204.
Lu, K., Li, T., He, J., Chang, W., Zhang, R., Liu, M., Yu, M., Fan, Y., Ma, J., Sun, W., Qu, C., Liu, L., Li, N., Liang, Y., Wang, R., Qian, W., Tang, Z., Xu, X., Lei, B., Zhang, K., Li, J., 2018. qPrimerDB: a thermodynamics-based gene-specific qPCR primer database for 147 organisms. Nucleic Acids Res. 46, D1229–D1236.
Machida, Y., 1965. Studies on the silk glands of silkworm, Bombyx mori L. I. Morphological and functional studies of Filippi's glands in the silkworm. Sci. Bull. Facul. Agric. Kyushu Univ. 22, 95–108.
Omenetto, F.G., Kaplan, D.L., 2010. New opportunities for an ancient material. Science 329, 528–531.
Patra, S., Singh, R.N., Raziuddin, M., 2012. Morphology and histology of Lyonet's gland of the tropical tasar silkworm, Antheraea mylitta. J. Insect Sci. 12, 1–7.
Sorour, J., Larink, A., Ramadan, A., Shalaby, A., Osman, S., 1990. Anatomical, histological and electron microscopical studies on the salivary glands of larvea of Spodoptera littoralis Boids (Lepidoptera: noctuidea). I. The anterior and posterior secretory parts. Zool. Jb. Anat. 120, 251–257.
Vepari, C., Kaplan, D.L., 2007. Silk as a biomaterial. Prog. Polym. Sci. 32, 991–1007.
Victoriano, E., Gregorio, E.A., 2004. Ultrastructure of the Lyonet's glands in larvae of Diatraea saccharalis Fabricius (Lepidoptera: Pyralidae). Biocell 28, 165–169.
Waku, Y., Sumimoto, K.I., 1974. Ultrastructure of Lyonet's gland in the silkworm (Bombyx mori L.). J. Morphol. 142, 165–185.
Wang, G.-H., Xia, Q.-Y., Cheng, D.-J., Duan, J., Zhao, P., Chen, J., Zhu, L., 2008. Reference genes identified in the silkwormBombyx moriduring metamorphism based on oligonucleotide microarray and confirmed by qRT-PCR. Insect Sci. 15, 405–413.
Wang, X., Li, Y., Liu, Q., Chen, Q., Xia, Q., Zhao, P., 2017a. In vivo effects of metal ions on conformation and mechanical performance of silkworm silks. Biochim. Biophys. Acta

1861, 567–576.
Wang, X., Li, Y., Liu, Q., Xia, Q., Zhao, P., 2017b. Proteome profile of spinneret from the silkworm. Bombyx mori. Proteomics 17.
Wang, X., Li, Y., Peng, L., Chen, H., Xia, Q., Zhao, P., 2016. Comparative transcriptome analysis of Bombyx mori spinnerets and Filippi's glands suggests their role in silk fiber formation. Insect Biochem. Mol. Biol. 68, 89–99.
Wu, Z.D., 1980. The Silkworm Anatomy and Physiology. Zhejiang agricultural university publishing house, Hangzhou.
Xia, J., Sinelnikov, I.V., Han, B., Wishart, D.S., 2015. MetaboAnalyst 3.0–making metabolomics more meaningful. Nucleic Acids Res. 43, W251–W257.
Xia, J., Wishart, D.S., 2010. MetPA: a web-based metabolomics tool for pathway analysis and visualization. Bioinformatics 26, 2342–2344.
Xia, Q., Li, S., Feng, Q., 2014. Advances in silkworm studies accelerated by the genome sequencing of Bombyx mori. Annu. Rev. Entomol. 59, 513–536.
Yi, Q.Y., Zhao, P., Wang, X., Zou, Y., Zhong, X.W., Wang, C., Xiang, Z.H., Xia, Q.Y., 2013. Shotgun proteomic analysis of the Bombyx mori anterior silk gland: an insight into the biosynthetic fiber spinning process. Proteomics 13, 2657–2663.
Zhang, Y., Hao, D., Liu, Z., Meng, P., Xu, F., 1997. The research on morphology of SG and FG of 18 species in Lepidoptera. J. Shenyang Agric. Univ. 28, 104–108 (in Chinese).
Zhou, L., Li, H., Hao, F., Li, N., Liu, X., Wang, G., Wang, Y., Tang, H., 2015. Developmental changes for the hemolymph metabolome of silkworm (Bombyx mori L.). J. Proteome Res. 14, 2331–2347.